Green Chemistry

Catalytic strategy for conversion of fructose to organic dyes, polymers, and liquid fuels

Journal:	*Green Chemistry*
Manuscript ID	GC-ART-05-2020-001576
Article Type:	Paper
Date Submitted by the Author:	07-May-2020
Complete List of Authors:	Chang, Hochan; University of Wisconsin Madison, Chemical and Biological Engineering Bajaj, Ishan; University of Wisconsin Madison, Chemical and Biological Engineering Huber, George; University of Wisconsin, Chemical and Biological Engineering Maravelias, Christos; University of Wisconsin Madison, Chemical and Biological Engineering Dumesic, James; University of Wisconsin Madison, Chemical and Biological Engineering

ARTICLE

Catalytic strategy for conversion of fructose to organic dyes, polymers, and liquid fuels

Received 00th January 20xx,
Accepted 00th January 20xx

DOI: 10.1039/x0xx00000x

Hochan Chang[a], Ishan Bajaj[a], George W. Huber[a], Christos T. Maravelias[a,b], and James A. Dumesic*[a,b]

We report a process to produce a versatile platform chemical from biomass-derived fructose for organic dye, polymer, and liquid fuel industries. An aldol-condensed chemical (HAH) is synthesized as a platform chemical from fructose by catalytic reactions in acetone/water solvent with non-noble metal catalysts (e.g., HCl, NaOH). Then, selective reactions (e.g., etherification, reduction, dimerization) of the functional groups, such as enone and hydroxyl groups, in the HAH molecule enable applications in organic dyes and polyether precursors. High yields of target products, such as 5-(hydroxymethyl) furfural (HMF) (85.9% from fructose) and HAH (86.3% from HMF) are achieved by sequential dehydration and aldol-condensation with a simple purification process (>99% HAH purity). The use of non-noble metal catalysts, the high yield of each reaction, and the simple purification of the target product allow for beneficial economics of the process. Techno-economic analysis indicates that the process produces HAH at minimum selling price (MSP) of $1958/ton. The MSP of HAH product allows the economic viability of applications in organic dye and polyether markets by replacing its counterparts, such as anthraquinone ($3200-$3900/ton) and bisphenol-A ($1360-$1720/ton).

Introduction

Biomass-derived platform chemicals have been considered to be promising renewable sources for supplying energy (liquid fuels) and chemicals. For example, 5-(hydroxymethyl) furfural (HMF) is one of the platform chemicals which can produce 2,5-dimethyl furan (DMF)[1] as a gasoline additive[2] or 2,5-furandicarboxylic acid (FDCA)[3] as a polymer precursor[4]. Biomass resources, such as glucose and fructose, have recently been shown to be converted to HMF in organic solvents[5]. Levulinic acid is another promising platform chemical which can be effectively synthesized from cellulose[6]. The levulinic acid can be converted to GVL[7] as a green solvent for diverse biomass upgrading processes[8–10] or for liquid fuel uses[11–13].

Recent decreases in liquid fuel prices and increases in demands of polymers and organic dyes have attracted interest in the production of high-value chemicals, which requires chemicals with high purity controlled functional groups in their molecular structure. For instance, organic dyes possess colorizing chemical features, called chromophores, such as aromatic (quinone dye) or ketone (C=O) functional groups to absorb the light in the visible and ultraviolet (UV) range[14]. Similarly, functional polymers utilize specific chemical functionalities, such as furan, α-ω diols or dicarboxyl acids, to improve the control over various polymer properties, such as thermal resistance[15], mechanical strength, and gas permeability[16,17]. Aldol-condensation is a chemical reaction that can append additional functional groups to a target molecule. Therefore, aldol-condensed chemicals can be used as new platform chemicals for applications in high-value chemicals by providing versatile functional groups[18,19].

However, important challenges must be addressed to develop a process to produce a versatile platform chemical from biomass that satisfy the markets of high-value chemicals (e.g., polymer, organic dye). Firstly, high purity of the platform chemical needs to be achieved from the process. This purity requirement can be associated with severe separation and/or purification steps that contribute high capital and operating costs. Secondly, the chemical stability of the platform chemical is required to prevent uncontrolled side-reactions, while promoting the desired reactions. An unstable platform chemical can lead to expensive cost of transportation and storage to minimize product degradation before selling. Lastly, hazardous solvents and noble metal catalysts that are typically used in biomass conversion need to be replaced by green solvents and inexpensive catalysts. The above challenges have confined biomass applications to be in liquid fuel industries since the fuels industries allow for chemical mixtures as final products, and the chemical stability of fuels is not of critical importance.

In this paper, we develop a catalytic strategy that enables a process for production of a new platform chemical (aldol-condensed product, HAH) from fructose, and we demonstrate the applications of the platform chemical for organic dyes and monomers. The proposed reaction route is described in Scheme 1. A high concentration (9.1 wt%) of fructose was dehydrated in acetone/water (75/25, v/v) solvent with HCl catalyst (60 mM) to produce a high yield (85.9%) of HMF. Then, the acetone solvent was evaporated under low temperature (~293 K) and pressure (~50 mbar) to minimize HMF degradation and prepare the appropriate molar ratio of HMF and acetone for aldol-condensation. The distilled solution, comprising HMF, acetone, HCl, and by-products, served as a feed for aldol-condensation without purification of HMF. A controlled amount of NaOH was used to neutralize HCl remaining from the dehydration step, and to catalyze the aldol-condensation. The initial molar ratio of the fructose-derived HMF and acetone determined the yield of the HAH product, up to the maximum yield of 83.6%. The difference in water solubility between the HAH

[a] Department of Chemical and Biological Engineering, University of Wisconsin–Madison, Madison, WI, USA. *Corresponding E-mail: jdumesic@wisc.edu
[b] DOE Great Lakes Bioenergy Research Center, University of Wisconsin-Madison, 1552 University Ave, Madison, WI 53726, USA.
Electronic Supplementary Information (ESI) available. See DOI: 10.1039/x0xx00000x

product and impurities allowed for simple purification of the HAH product by washing with water. ^{1}H NMR and ^{13}C qNMR spectra were used to characterize the HAH molecule, and the purity of HAH product was measured to be >99% by HPLC analysis. The functional groups, such as diols and enones, in HAH were selectively converted by etherification, dimerization, and reduction reactions to demonstrate applications in organic dye and polymer industries. Furthermore, techno-economic analysis (TEA) assessed the economic viability of the process. The minimum selling price (MSP) of HAH product was calculated to be $1958/ton and it suggests that anthraquinone ($3200-$3900/ton) and bisphenol-A ($1360-$1720/ton) would become potential markets for replacement by HAH. This production process of the new biomass-derived platform chemical provides new directions for utilizing a sustainable resource in various high-value chemicals markets.

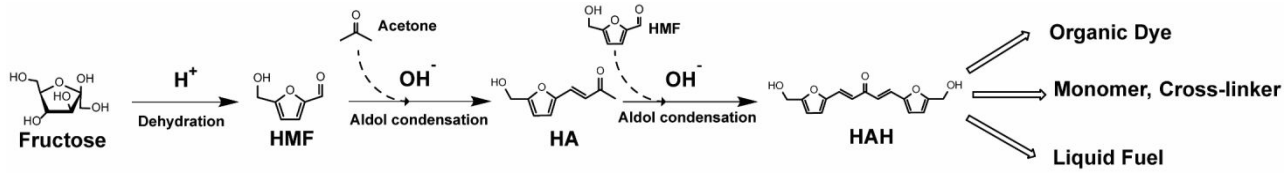

Scheme 1. Overall catalytic reaction route for HAH production from fructose by dehydration and aldol-condensation.

Results and Discussion

Solvent effect on fructose dehydration to HMF

The acetone-rich solvent was shown to enhance the fructose dehydration reactivity (Fig.1.A). 0.6 g of fructose was dehydrated in 8 mL of acetone/water solvent with different acetone composition over Amberlyst-15 catalyst. Fructose conversion and HMF yield increased from 38.5% to 71.3% and from 34.7% to 60.1%, respectively, as the acetone/water volume ratio increased from 50% to 70% after 150 min dehydration at 393 K. 91.3% fructose was converted to HMF in 78.7% yield at 393 K and 90 min dehydration in acetone/water (80/20, v/v) solvent. HMF selectivity was >76.8% and remained stable in the acetone/water solvent. Therefore, the fructose dehydration reaction demands the utilization of an acetone-rich solvent (>70 vol% acetone) to maximize the HMF production rate.

Previous work reported that homogeneous acids are effective catalysts for fructose dehydration in the acetone-rich solvent[5]. In this respect, Amberlyst-15 catalyst was replaced with HCl to optimize the HMF yield and carbon balance in the dehydration step. Moreover, the solubility of fructose defined the upper limitation of the fructose concentration as a feed. The fructose solubility decreased from 80.0 wt% to 8.3 wt% (Fig.S1) by adjusting the solvent from pure water to acetone/water (80/20, v/v) mixture at 298 K. Operating a reaction at the upper limitation of the feed concentration results in a higher production rate of the target product (HMF). When fructose dehydration was performed at 393 K for 100 min in an acetone/water (50/50, v/v) solvent containing 137mM HCl, fructose was almost completely converted (94.0%), resulting in 49.7% HMF yield and 67.3% carbon balance (Fig.1.B). However, the fructose conversion, HMF yield, and carbon balance increased to 98.6%, 88.8%, and 94.2%, respectively, when the reaction was conducted at 393 K for 30 min in an acetone/water (75/25, v/v) solvent containing 121 mM HCl (Fig.1.C). The decrease in water content of the polar aprotic/water co-solvent improved the catalytic turnover rates towards the target products that were catalyzed by acid[20]. Therefore, an appropriate amount (75 vol%) of acetone was used as the solvent for fructose dehydration because addition of acetone leads to higher HMF yield and carbon balance while it decreases the fructose solubility.

During fructose dehydration, a minor acid-catalyzed aldol-condensation was observed, leading to formation of HA. Thus, the dehydrated solution mainly contained HMF, HA, and acidic by-products (formic acid, levulinic acid) after the dehydration step (Fig.1.D). Fructose was also converted to sugar isomers (mannose, anhydro-sugar, cellobiose). 3.6% of the carbon of the fructose feed was converted to humins that must be removed before further processing to minimize the acid-catalyzed side-reactions[21]. In Fig.1.D, activated carbon selectively adsorbed the humins without significant changes in concentrations of other chemicals. A minor increase in HMF concentration (Fig.1.D) after the humin removal resulted from the measurement error of HPLC by acetone evaporation during the activated carbon treatment.

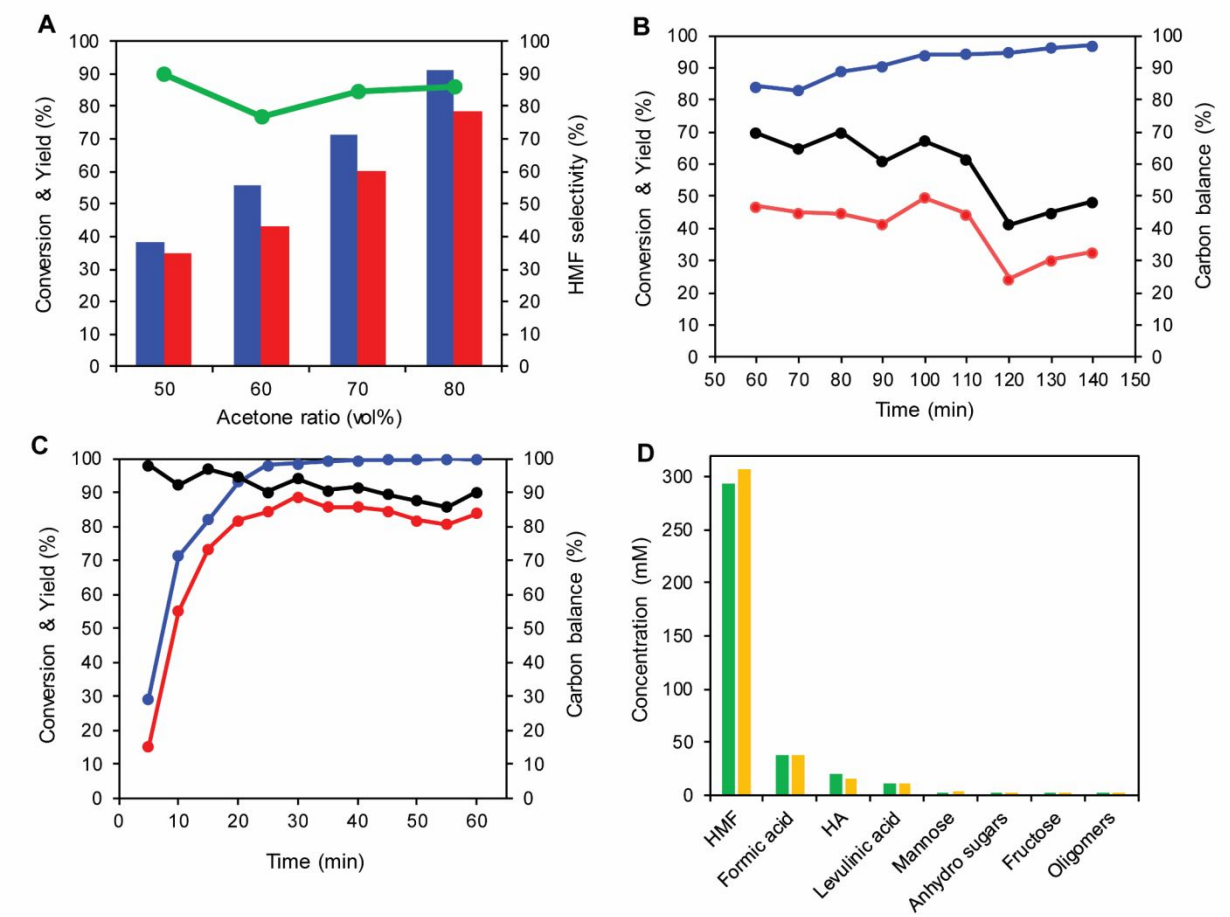

Fig.1. (**A**) Fructose conversion (Blue bar), HMF yield (Red bar), and HMF selectivity (Green dot) as a function of acetone ratio in the solvent (Reaction conditions: 0.6 g fructose (~420 mM) in 8 mL acetone/water solvent at 393 K over 0.2 g Amberlyst-15 catalyst), (**B**) Fructose conversion (Blue), HMF yield (Red), and Carbon balance (Black) as a function of reaction time (Reaction conditions: 19.6 wt% fructose in acetone/water (50/50, v/v) solvent with 137 mM HCl), (**C**) Fructose conversion (Blue), HMF yield (Red), and Carbon balance (Black) as a function of reaction time (Reaction conditions: 9.1 wt% fructose in acetone/water (75/25, v/v) solvent with 121 mM HCl), (**D**) Chemicals concentration in dehydrated solution before (Green bar) and after (Yellow bar) the decolorization (Decolorization conditions: 1.7 wt% activated carbon and 23 wt% water were mixed with dehydrated solution at 298 K for 30 min.

HMF degradation during vacuum distillation

The distillation of acetone solvent was used to control the molar ratio of HMF and acetone for selective production of HAH by aldol-condensation. Excess amounts of acetone produce HA as a major product from aldol-condensation of fructose-derived HMF and acetone[19]. Acid-catalyzed degradation of HMF and HA was observed after vacuum distillation at 298 K, 50 mbar. 9.6% of HMF loss and 10% of HA loss were measured by analyzing the distilled solution (Table S1). 14% formic acid was accumulated during the humin formation by degradation of HMF and HA, which is consistent to previous reports[22]. HMF degradation was suppressed (from 10±5% to 6±3%) by reducing the amount of HCl catalyst (from 120 mM to 60mM) in the dehydration step, adding water to dilute HCl before the distillation, and decreasing the distillation temperature (from 298 to 293 K). With reduced concentration of HCl catalyst (60 mM), 9.1 wt% fructose in acetone/water (75/25, v/v) solvent resulted in the high HMF yield (85.9%) and carbon balance (96.4%). The major three compounds of the distilled HMF solution were HMF, acetone, and formic acid (Fig.2). As a result, the HMF yield from fructose slightly decreased (from ~85.9% to ≤83.2%) by acid-catalyzed degradation in the distillation step.

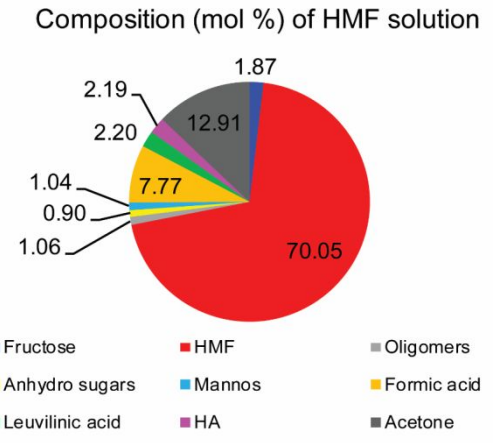

Fig.2. Molar composition of HMF solution (feed for aldol-condensation) after the fructose dehydration, humin decolorization, and acetone distillation.

Aldol-condensation of fructose-derived HMF and acetone

The fructose-derived HMF solution was acidic because it contained acidic by-products (e.g., formic acid, levulinic acid) and HCl catalyst from the dehydration step. Therefore, addition of the controlled amount of NaOH is necessary to neutralize the acids and catalyze the aldol-condensation. Each concentration of acidic by-product was measured by HPLC, and the concentration of HCl was assumed to be the same as the initial addition in the dehydration step because water solvation prevented the vaporization of HCl[23] in the distillation step. The yield of HAH and HA depended on the initial molar ratio of HMF to acetone sources ($\frac{\text{HMF}}{\text{Acetone + HA}}$). The highest HAH yield from the fructose-derived HMF was 86.3% with 93.0% carbon balance when $\frac{\text{HMF}}{\text{Acetone + HA}}$ (mol) ratio was 2.5 (Fig.3).

Previous work on the aldol-condensation of furfurals and ketones reported that the presence of neutral salts does not affect the reaction kinetics of aldol-condensation[24]. Thus, while sugar isomers and humins are possible impurities that can cause side-reactions in aldol-condensation step, the acidic by-products should not cause side-reactions by forming the neutral salts (sodium formate, sodium levulinate) before the aldol-condensation. Humin-free feed for aldol-condensation was prepared by decolorization of the feed over activated carbon to investigate the effect of humins on side-reactions. There was no significant difference in HAH yield and carbon balance between humin-free feed (Decolorized feed) and humin-containing feed (Untreated feed) (Fig.S2.A). This result indicates that the presence of sugar isomers affected the loss (7.0%) in the carbon balance during aldol-condensation. Previous research about the formation of carbohydrate complexes from alkaline degradation of fructose and glucose[25] supports the idea that the sugar isomers induced humin formation. Moreover, acid-catalyzed degradation of HMF and HA was observed during decolorization at 298 K (Fig.S2.B). Accordingly, decolorization of the feed has no benefit for production of HAH.

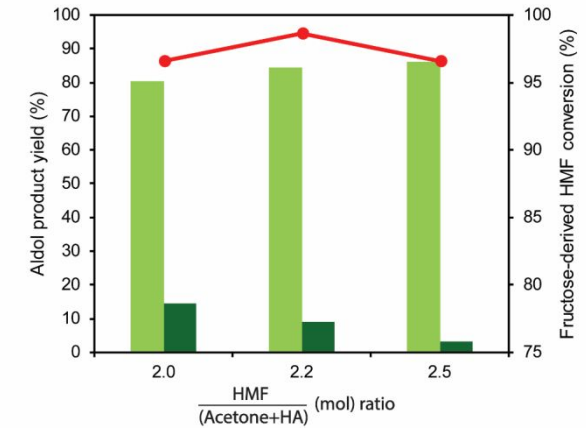

Fig.3. Aldol-product yield (HAH: Light green bar, HA: Dark green bar) and fructose-derived HMF conversion (Red dot) as a function of $\frac{HMF}{Acetone\ + HA}$ (mol) ratio (Reaction conditions: 0.12 M (70 min), 0.23 M (60 min), 0.21 M (60 min) NaOH for $\frac{HMF}{Acetone\ + HA}$ (mol) = 2.0, 2.2, 2.5 at 308 K).

Crystallization and purification of HAH

The fructose-derived HAH spontaneously crystallized during the aldol-condensation due to its low solubility in water[19]. The water solubility of residual HMF, HA, salts (NaCl, sodium formate, sodium levulinate), and humins was higher than the HAH solubility. 6.2% of the produced HAH was dissolved in water with the water-soluble impurities and discarded with the purge stream after the purification. >99% purity of the purified HAH was measured by HPLC analysis (Fig.S9.C). The spontaneous crystallization enables a simple and inexpensive purification to produce high yield (80.9%) of purified HAH from fructose-derived HMF.

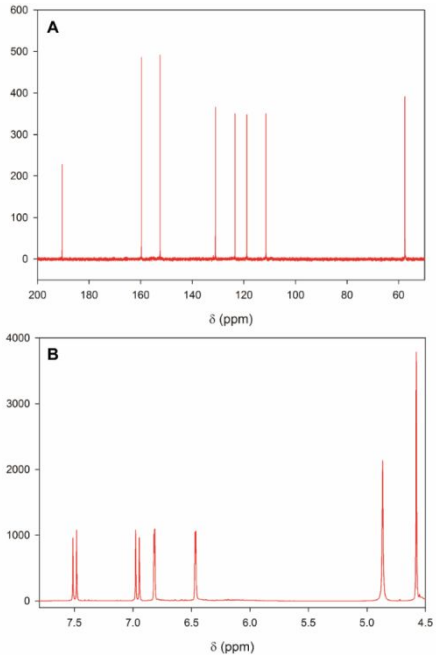

Fig.4. (**A**) ^{13}C quantitative NMR (qNMR) spectrum of purified, fructose-derived HAH (126 MHz, MeOD) δ: 190.49 (1C), 159.65 (2C), 152.51 (2C), 131.01 (2C), 123.42 (2C), 118.84 (2C), 111.42 (2C), 57.61 (2C) ppm, (**B**) ^{1}H standard NMR spectrum of purified, fructose-derived HAH (500 MHz, MeOD) δ: 7.51 (s, 1H), 7.48 (s, 1H), 6.98 (s, 1H), 6.95 (s, 1H), 6.82 (d, 2H), 6.47 (d, 2H), 4.58 (s, 4H) ppm (MeOD: 4.87 (s) ppm).

Selective conversion of functional groups in HAH for organic dye and polymer applications

The reactivity of diol functional group in HAH was investigated by the etherification of HAH with methanol. 93.9% conversion of HAH and the corresponding yield of the etherifed HAH were measured by ^{13}C qNMR analysis after 9h reaction over a WO_x-ZrO_2 catalyst at 453 K in methanol solvent. The Lewis and Br*ϕ*nsted acid sites of the catalyst acted as catalytic active sites for etherification[26,27]. The etherification of HAH was highly effective since minimal formation of by-products (< 4.5 carbon%) was detected by ^{13}C qNMR spectrum. The effective etherification of diol groups in HAH suggests that HAH is a candidate for polyether precursors in the presence of acid catalyst. In addition, the carbonyl group of HAH was converted to a secondary alcohol by selective reduction with the reduction agent, $NaBH_4$. >95% conversion of HAH and the corresponding yield of the selectively

reduced HAH were measured by ^{13}C qNMR analysis. The symmetric structure and tri-hydroxy group (two primary and one secondary alcohol groups) in the selectively reduced HAH enables a cross-linker application, like glycerol.

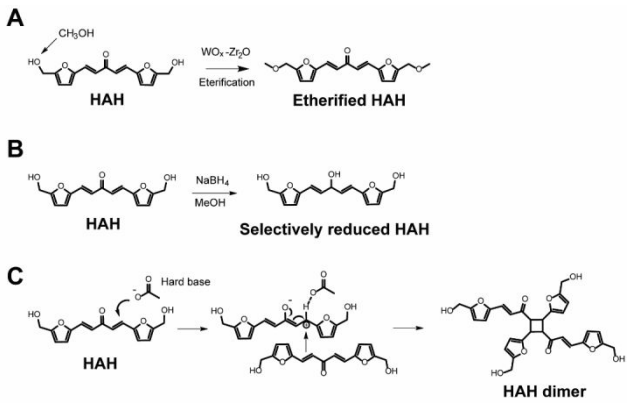

Scheme 2. Reaction mechanism of (**A**) HAH etherification with methanol over WO_x-ZrO_2 catalyst, (**B**) HAH selective reduction in presence of $NaBH_4$, and (**C**) HAH dimerization with acetate anion.

An adjustable UV-vis absorption band and high molar excitation coefficient of the molecule are of critical importance for organic dye applications. The HAH molecule had a broad absorption spectrum from two chromophores, 2-hydroxymethyl furan and 1,4-pentadien-3-one, shown as (i) and (ii), respectively (Fig.5.A). Shifts in the absorption spectrum of HAH were achieved by dimerization and etherification (Fig.5.A). The dimerization ([2+2] cycloaddition) tuned the (ii) moiety (marked in Fig.5.A) in HAH and produced a HAH dimer at room temperature for 8 days in the presence of acetate anion as a hard base. 94.3% yield of HAH dimer from HAH was measured by ^{13}C qNMR analysis after the dimerization. The HAH dimer yielded a narrow UV-vis absorption spectrum by shifting the maximum absorption wavelength from 378 nm (by HAH) to 334 nm. Similarly, etherification eliminated the (i) moiety (marked in Fig.5.A) in HAH and resulted in a sharp absorption band at 378 nm as the maximum absorption wavelength. The molar excitation coefficient of HAH in methanol solvent was measured to be 22,262 $M^{-1}{\cdot}cm^{-1}$ at 378 nm incident UV light (Fig.5.B). This value of HAH is within the range of typical molar excitation coefficients (from 2,900 to 43,000 $M^{-1}{\cdot}cm^{-1}$) of organic dyes, monosubstituted anthraquinones, in methanol solvent at UV incident light[28]. Note that HAH effectively absorbs UV light (from 300 to 450 nm) and can thus serve as a functional organic dye to protect materials from UV light.

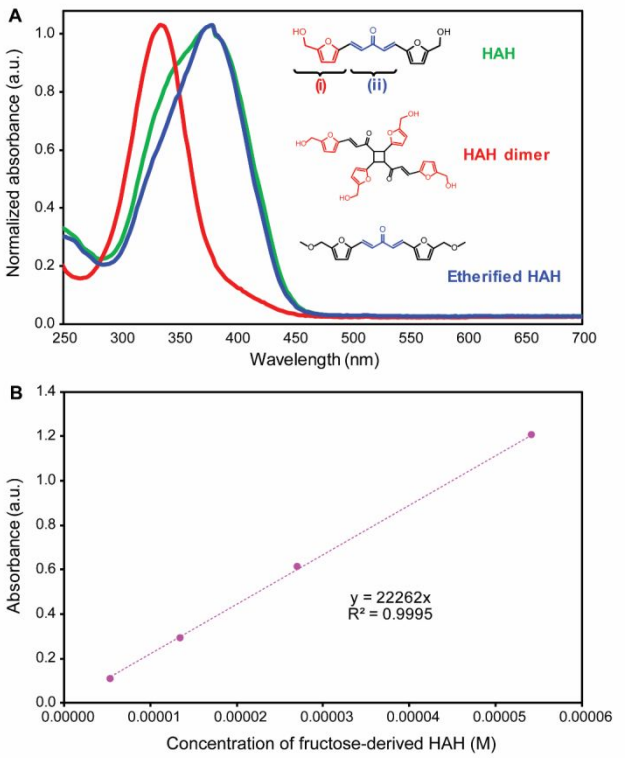

Fig.5. (A) UV-vis absorption spectrum of diluted HAH (Green), HAH dimer (Red), and etherified HAH (Blue) in methanol solvent. (i) (2-hydroxymethyl furan) and (ii) (1,4-pentadien-3-one) represent the chromophores of HAH. (**B**) Molar excitation coefficient (slope, $M^{-1}cm^{-1}$) of diluted fructose-derived HAH in methanol solvent at 378 nm UV incident light.

Techno-economic model analysis of HAH production process

We developed a process model for the conversion of fructose to HAH (Fig.6) based on the aforementioned experimental data in Aspen Plus. Then, we performed techno-economic analysis (TEA) for the base design, based on fructose flow rate of 10,000 $kg{\cdot}h^{-1}$. A detailed description of the process is provided in the experimental methods and supplementary information, with the process flow diagram shown in Fig.S10. Other pertinent information required to estimate the minimum selling price (MSP) of HAH are given in Tables S4-S6. If the price of fructose is assumed to be \$650/ton, the analysis suggests that HAH can be produced using the proposed process at an MSP of \$1958/ton (Fig.7). The high yields of HMF and HAH, and the ease of their separation from the solvent lead to favorable economics. The costs of the feedstock (67%) and acetone (14%) are the biggest contributors to the MSP of HAH. Reducing the price of the feedstock and increasing the plant capacity reduces the MSP of HAH (Fig.S11). For instance, if the price of fructose is reduced to \$500/ton, then the MSP of HAH is estimated to be \$1675/ton. The results indicate that HAH can be a sustainable and economically competitive alternative to fossil fuels-derived polyether monomer, bisphenol-A (\$1360-\$1720/ton)[29] and organic dye, anthraquinone (\$3200-\$3900/ton)[30].

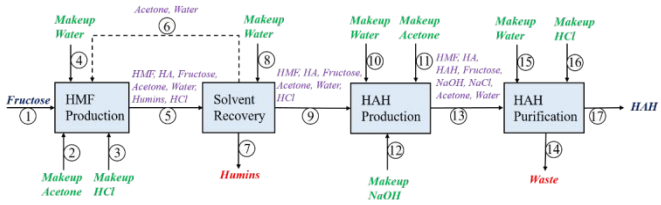

Fig.6. Overview of the process block-flow diagram to produce HAH from fructose.

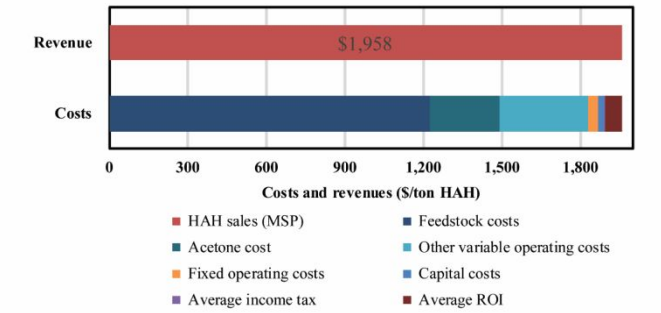

Fig.7. Breakdown of the costs and revenue of the proposed approach.

Conclusion

We designed a process for production of a biomass-derived platform chemical (HAH) by optimizing the catalytic reactions, using green solvents, non-noble metal catalysts, and a simple purification strategy. The acetone/water (75/25, v/v) solvent with low concentration of HCl (60 mM) catalyst allowed for production of HMF in high yield (85.9%) from a high concentration fructose (9.1 wt%) feed. Acetone distillation following HMF production was used to provide a controlled molar ratio of HMF and acetone, with minimal HMF degradation. High yield (86.3%) of HAH from the fructose-derived HMF was achieved by aldol-condensation of the feed with the controlled molar ratio of the reactants ($\frac{\text{HMF}}{\text{Acetone + HA}}$=2.5). The acidic by-products (e.g., formic acid, levulinic acid) and HCl were converted to salts by neutralization before aldol-condensation to minimize side-reactions in the aldol-condensation step. The HAH product was purified simply (>99% purity) by washing with water due to its low solubility in water. The applications of HAH were demonstrated by selective conversion of the functional groups in HAH molecules. The diol in HAH was etherified by methanol over a WO_x-ZrO_2 catalyst, suggesting that HAH can be a candidate for the polyether precursors. Selective reduction of the carbonyl group in HAH produced a chemical with tri-hydroxy group, which can be used as a cross-linker for polymer applications. Furthermore, two HAH molecules were dimerized in the presence of acetate anion, leading to a shift in the UV-vis absorption spectrum. The high molar excitation coefficient (22,262 $M^{-1}\cdot cm^{-1}$) and the adjustable UV-vis absorption band of HAH molecule enable uses for HAH as a suitable candidate for an organic dye. Finally, techno-economic analysis of the process was employed to evaluate the effectiveness of the process by comparing the minimum selling price of HAH product with market prices of current counterparts from petroleum. The minimum selling price of HAH ($1958/ton), calculated at the production rate less than the volume of the potential markets, suggests that the HAH product could replace current markets of organic dyes (anthraquinone market price: $3200-$3900/ton) and polyethers (bisphenol-A market price: $1360-$1720/ton). This biomass-derived platform chemical from the optimized process could thus supply organic dyes, polymers, and liquid fuels from renewable sources in the future.

Experimental methods

Materials

Fructose (>99%, Sigma-Aldrich), acetone (HPLC grade, Fisher Scientific), methanol (HPLC grade, Fisher Scientific), NaOH (FCC specification, Fisher Scientific), HCl (6N, Fisher Scientific), activated carbon (Norit SX-Ultra), HMF (98% AK Scientific), and Mill-Q water (~18 MΩ cm) were used in all the experiments. Commercial tungstated zirconium hydroxide (15 wt% WO_3 loading, MEL Chemicals, XZO1251/01), sodium borohydride (Sigma-Aldrich, purum p.a. >96%), sodium acetate (Sigma-Aldrich), ethyl acetate (HPLC grade, Fisher Chemical), hexane (HPLC grade, Sigma-Aldrich), etherification reaction was performed in a 50 mL Parr reactor (Parr Instrument Company).

Decolorization of the dehydrated solution on activated carbon

Activated carbon was received from Cabot Corporation and used as received. The humins from fructose dehydration were selectively adsorbed on activated carbon at 298 K. In a milligram scale experiment, 0.35 g activated carbon was added to 7.4 g dehydrated solution and stirred for 30 min. After the adsorption, activated carbon was filtrated through 0.2 µm PTFE filter. In a gram-scale experiment, 13.4 g water was added to 57 g dehydrated solution to dilute HCl concentration before activated carbon adsorption. Then, 1 g activated carbon was added to 70.4 g diluted solution and stirred for 30 min. After the adsorption, activated carbon was removed by filtration of the solution through filter paper (Grade 50 filter, Whatman). 0.1 mL of the filtered solution was diluted 10 times with Milli-Q water and analyzed using HPLC (Aminex HPX-87H column, Bio-Rad) to measure the concentrations of fructose, HMF, sugar isomers, and acidic by-products (formic acid, levulinic acid). 0.1 mL of the filtered solution was diluted 5 times with methanol and analyzed using HPLC (Luna C18 column, Phenomenex) to measure the concentration of HA.

Vacuum distillation of dehydrated and decolorized product

The decolorized solution was distilled under ~100 mbar in the air (~298 K). Acetone was evaporated before water under ~100 mbar while the temperature of the solution decreased from 298 K to 290 K during acetone evaporation. After acetone evaporation, the pressure was further decreased from ~100 to ~50 mbar to evaporate water. During the water evaporation in the air, the temperature of the solution was around 290-293 K. The density of decolorized solution increased from 0.922 g/mL to 1.027 g/mL. The density of the solution was always more than 1.02 g/mL when $\frac{HMF}{Acetone + HA}$ (mol) > 2.

HPLC analysis of dehydrated, decolorized, and distillated solution

The chemical composition of the dehydrated, decolorized, and distillated solution was quantified by High Performance Liquid Chromatography (HPLC) analysis. 0.1 mL of dehydrated or decolorized solution was diluted 10 times with Milli-Q water for analyzing the concentration of fructose, HMF, sugar isomers, and acidic by-products (formic acid, levulinic acid). Similarly, 0.1 mL of dehydrated or decolorized solution was diluted 5 times with methanol for analyzing the concentrations of HMF and HA. 0.04 mL of distilled solution was diluted 20 times with Milli-Q water for analyzing the concentrations of acetone, sugars, HMF, and acidic by-products. Similarly, 0.04 mL of distilled solution was diluted 10 times with methanol for analyzing the concentrations of HMF and HA. All the diluted samples were filtrated through 0.2 μm PTFE filter before the sample was injected into HPLC. The concentrations of fructose, sugar isomers, and acidic by-products were measured by a Water 2695 separation module equipped with a Aminex HPX-87H (Bio-Rad) column and RI detector, while HMF concentration was measured with a Waters 2998 PDA detector at 320 nm. The temperature of the HPLC column was maintained at 338 K, and the flow rate of the mobile phase (pH 2 water, acidified by sulfuric acid) was 0.6 mL min^{-1}. The concentration of HA was measured by a Water 2695 separation module equipped with a Luna C18 (Phenomenex) column and a Waters 2998 PDA detector set at 390 nm (for HA analysis). The temperature of the HPLC column was held constant at 323 K. The mobile phase was a gradient of methanol/water (with 0.1 wt% formic acid) at a constant flow rate of 1.0 mL min^{-1} (0.1 wt% formic acid water linearly changed to methanol in 20 min, held pure methanol for 7 min, and methanol linearly changed to 0.1 wt% formic acid water in 3 min).

$$\text{HMF yield from fructose} = \frac{\text{Moles of final HMF}}{\text{Moles of initial fructose}} \cdot 100\ (\%) \qquad (1)$$

$$\text{Fructose conversion} = \frac{\text{Moles of initial fructose} - \text{Moles of final fructose}}{\text{Moles of initial fructose}} \cdot 100\ (\%) \qquad (2)$$

HPLC analysis of aldol-condensed solution

After aldol-condensation, residual HMF and aldol-condensed products (HA, HAH) were quantified by HPLC analysis. The as-synthesized solution was neutralized with HCl (pH of the solution was measured by pH test strips) and diluted 4 times with methanol to terminate aldol-condensation and dissolve precipitated HAH. 0.1 mL of diluted solution was further diluted 10 times with methanol for analyzing the concentrations of HMF and HA. Similarly, 0.01 mL diluted solution was diluted 500 times with methanol for analyzing the concentration of HAH to avoid the signal saturation of the PDA detector. The diluted samples were filtrated through 0.2 μm PTFE filter before the sample was injected into HPLC. The concentrations of HMF, HA, and HAH were measured by a Water 2695 separation module equipped with a Luna C18 (Phenomenex) column and a Waters 2998 PDA detector, set at 320 nm (for HMF analysis) and 390 nm (for HA, HAH analysis). The temperature of the HPLC column and mobile phase were same as described above. Purified chemical standards of HA and HAH were used for the calibration of concentration and integrated peak area.

$$\text{HA yield from HMF} = \frac{\text{Moles of final HA}}{\text{Moles of initial HMF}} \cdot 100\ (\%) \qquad (3)$$

$$\text{HAH yield from HMF} = \frac{2 \cdot \text{Moles of final HAH}}{\text{Moles of initial HMF}} \cdot 100\ (\%) \qquad (4)$$

$$\text{HMF conversion} = \frac{\text{Moles of initial HMF} - \text{Moles of final HMF}}{\text{Moles of initial HMF}} \cdot 100\ (\%) \qquad (5)$$

Fructose dehydration with HCl in acetone/water (75/25, v/v) solvent

In a milligram-scale experiment, aqueous feed (25 wt% fructose) was prepared by dissolving 5 g fructose and 1.26 mL of 3 M HCl solution in 13.74 mL Milli-Q water. 2.69 g aqueous feed (0.67 g fructose, 2 mL water, 0.02 g HCl) was mixed with 6 mL acetone in a 10 mL thick-walled glass reactor (Chemglass). A triangular stir bar was added for stirring at 700 rpm. The reactor was placed in an oil bath at 393 K for 75 min. In a gram scale experiment, 4 g fructose and 1.16 g of 3 M HCl were dissolved in 11 g Milli-Q water to prepare the aqueous feed. Then, 35.63 mL acetone was mixed with the aqueous feed in a 48 mL thick-walled glass reactor (Ace glass). An egg-shaped stir bar was added for stirring at 900 rpm. The reactor was placed in an oil bath at 393 K for 95 min. The dehydration was terminated by cooling the reactor in a water bath.

Fructose dehydration with HCl in acetone/water (50/50, v/v) solvent

The aqueous feed (30 wt% fructose in water) was prepared by dissolving 6.5 g fructose and 0.75 mL 6 M HCl solution in 14.25 mL Milli-Q water. 5.07 g aqueous feed (1.53 g fructose, 3.5 mL water, 0.04 g HCl) was mixed with 3.5 mL acetone in a 10 mL thick-walled glass reactor (Chemglass). A triangular stir bar was added for stirring at 790 rpm. Each reactor was placed in an oil bath at 393 K for different reaction times. The dehydration was terminated by cooling the reactor in a water bath. 0.5 mL dehydrated sample was diluted 10 times with Milli-Q water and analyzed using HPLC (Aminex HPX-87H column, Bio-Rad) to measure the concentration of fructose, HMF, sugar isomers, and acidic by-products. The HPLC sample was filtrated with 0.2 μm PTFE filter before the sample injection into HPLC.

Fructose dehydration in different ratios of acetone/water solvent over Amberlyst-15

For acetone/water (50/50, v/v) solvent experiments, 0.6 g fructose was dissolved in the mixture of 4 mL Milli-Q water and 4 mL acetone. For acetone/water (60/40, v/v) solvent experiments, 0.6 g fructose was dissolved in the mixture of 3.2 mL Milli-Q water and 4.8 mL acetone. For acetone/water (70/30, v/v) solvent experiments, 0.6 g fructose was dissolved in the mixture of 2.4 mL Milli-Q water and 5.6 mL acetone. For acetone/water (80/20, v/v) solvent experiments, 0.54 g fructose was dissolved in the mixture of 1.6 mL Milli-Q water and 6.4 mL acetone. 0.2 g Amberlyst-15 catalyst was added to the fructose feed and the reactor was placed in an oil bath at 393 K. A triangular stir bar was used for stirring at 650 rpm. 150 min reaction time was used for the experiments of 50/50, 60/40, and 70/30 acetone/water solvents. 90 min reaction time was used for 80/20 acetone/water solvent experiment since the fructose conversion had reached near the complete conversion. 10 mL thick-walled glass reactors (Chemglass) were used for the experiments. The dehydrated solution was decolorized on 0.06 g activated carbon for 30 min before HPLC analysis. 0.5 mL decolorized sample was diluted 10 times with Milli-Q water and filtrated with 0.2 μm PTFE filter before the sample injection into HPLC.

Table.1 Fructose dehydration in different acetone/water solvents.

Solvent volume composition (acetone/water)	Fructose added (g)	Amberlyst-15 added (g)	Milli-Q water added (mL)	Acetone added (mL)	Reaction time (min)
50/50	0.60	0.20	4.0	4.0	150
60/40	0.60	0.20	3.2	4.8	150
70/30	0.60	0.20	2.4	5.6	150
80/20	0.54	0.20	1.6	6.4	90

Aldol-condensation of fructose-derived HMF and acetone

The concentrations of the distilled solution containing reactants (HMF, acetone, HA) and acidic by-products (formic acid, levulinic acid) were measured by HPLC analysis and this solution was used as a feed for aldol-condensation. The appropriate amount of acetone was added to the distillated solution for various initial $\frac{HMF}{Acetone+HA}$ experiments. Similarly, the appropriate amount of 3 M NaOH solution was determined based on previous kinetic model [19] and the amount required to neutralize the acids (HCl, formic acid, levulinic acid) in the distilled solution. The required amount of NaOH solution was added to the feed solution, containing a specific molar ratio of HMF and acetone sources ($\frac{HMF}{Acetone+HA}$), at room temperature and then the solution was placed in an oil bath at 308 K. The cross-shaped stir bar was used for stirring at 475 rpm. The reaction time was determined by the kinetic model [19] to maximize the HAH yield. The product solution was neutralized with 0.5 M HCl solution and diluted with methanol for HPLC analysis.

Table 2. Feed conditions and reaction time for various initial molar ratio of HMF and acetone source

$\frac{\text{HMF}}{\text{Acetone + HA}}$ (mol)	Acetone added (g)	3 M NaOH solution added (mL)	HMF in distillated solution (g)	HA in distillated solution (g)	Acetone in distillated solution (g)	Reaction time (min)
2.0	0.0100	0.400	0.310	0.010	0.030	70
2.2	0.0000	0.175	0.094	0.004	0.018	60
2.5	0.0075	0.173	0.096	0.004	0.016	60

Purification of HAH by water washing filtration

As-synthesized HAH from aldol-condensation of fructose-derived HMF and acetone was purified by spontaneous crystallization in water. The aldol-condensed solution was neutralized by HCl before the purification. The neutralized solution was washed by passing water slowly during the paper filtration, leading to HAH precipitation and removal of water-soluble impurities (HMF, HA, salt, sugars). After collecting the washed HAH, the solid state of purified HAH was dried at 323-333 K overnight (>18 h) to remove residual water. The purity of the dried HAH was analyzed by HPLC and the molecular structures of HAH was characterized by ^{1}H and ^{13}C NMR spectrum (Fig.4).

Preparation of HA chemical standard by column chromatography

89 mg of commercial HMF was dissolved in a solution containing 0.5 ml acetone and 0.48 ml Milli-Q water in a 10 mL glass vial. A cross-shaped stir bar was added to the glass vial for mixing and the solution was heated to 308 K in an oil bath. The solution was kept at 308 K for 15 min before the addition of NaOH to reach thermal equilibrium. 0.135 ml of 1 M NaOH solution was injected to the HMF solution and the solution was stirred (800 rpm) at 308 K for 10 min. After the required time had elapsed, 1.11 ml of 0.1 M HCl solution was added to the product solution to terminate aldol-condensation. Column chromatography isolated HA and produced a standard chemical for HPLC quantification. Prior to chromatography, water solvent was evaporated at 313 K, under 50 mbar from the product mixture obtained after aldol-condensation. The concentrated product solution was separated by passing it through a silica gel column. Ethyl acetate/hexane mixture (50/50 (v/v)) was used as the eluent. Purified HA solution (light yellow liquid) was collected. Ethyl acetate and hexane were evaporated at 313 K under 200 mbar. The purity of HA was determined by ^{1}H and ^{13}C NMR spectrum (Figure S3). The purified HA was used as the calibration standard for HPLC analysis.

Preparation of etherified HAH

6 g commercial tungstated zirconium hydroxide was calcined at 923 K for 3 h in a muffle furnace. The temperature was raised from room temperature to 923 K with 5 K·min^{-1} ramping rate. 31 mg calcined WO_x-ZrO_2 catalyst was placed in a 50 mL Parr reactor. 153 mg of HAH was completely dissolved in 10 mL methanol to prepare the feed. The HAH solution in methanol (56 mM) was added in the Parr reactor. The reactor was purged twice with 20 bar Ar to displace the air in the reactor. Then, 20 bar Ar was filled into the reactor for the etherification at room temperature. The Parr reactor was heated to 453 K in 1 h (final pressure increased to 55 bar at 453 K). The reactor was kept at 453 K for 9 h with 450 rpm stirring speed, and then cooled to room temperature by natural convection. The solid catalyst was separated from the etherified HAH by filtration. The methanol solvent was evaporated under 100 mbar at 313 K and the product was characterized by ^{1}H NMR, ^{13}C quantitative NMR, and high-resolution mass spectrometry (HRMS) (Fig.S.4). The conversion and yield were measured by ^{13}C quantitative NMR spectrum.

Preparation of selectively reduced HAH

137 mg HAH was dissolved in 10mL methanol solvent to prepare the feed solution. 38 mg $NaBH_4$ was added in the HAH solution with vigorous stirring for 2 h at arbitrary room temperature. 30 mL ethyl acetate and 10 mL saturated NaCl solution in water were added into

the reduced HAH solution for the extraction. The organic phase was separated and evaporated under 150 mbar at 313 K and the product was characterized by ^{1}H NMR, ^{13}C quantitative NMR, and high-resolution mass spectrometry (HRMS) (Fig.S.5). The conversion and yield were measured by ^{13}C quantitative NMR spectrum.

Preparation of HAH dimer

50 mg of HAH was mixed with 5 mL water and sonicated to produce colloidal dispersion. 60 mg of sodium acetate was added to the HAH colloidal solution. The colloidal HAH solution was vigorously stirred for 8 days at arbitrary room temperature. The dimerized product was precipitated by centrifugation (3000 rpm, 10 min) and the aqueous phase was gently separated by using pipette. The precipitated product was evaporated under 50 mbar at 313 K and the product was characterized by ^{1}H NMR, ^{13}C quantitative NMR, and high-resolution mass spectrometry (HRMS) (Fig.S.6). The conversion and yield were measured by ^{13}C quantitative NMR spectrum.

UV-vis absorption spectrum of HAH, HAH dimer, and etherified HAH

HAH, HAH dimer, and etherified HAH were diluted in methanol solvent until the absorbance signals of the detector were not saturated. 12 mg of fructose-derived HAH was dissolved in 40 mL of methanol solvent to prepare the parent HAH solution (~0.001M) for molar excitation coefficient measurement. The parent HAH solution (~0.001M) was further diluted in methanol solvent to prepare 0.000054, 0.000027, 0.000014, and 0.000005M HAH solution. All diluted samples were placed to absorption glass cell (Fisherbrand, Absorption Macro Special Optical Glass) and measured by UV-vis spectrophotometer (Beckman Coulter, DU-520). Pure methanol solvent was scanned for background signal from 250 to 700 nm.

Techno-economic analysis

To demonstrate the economic feasibility of the approach, the minimum selling price (MSP) of HAH was computed. The techno-economic analysis follows four steps. First, we design a process to convert fructose to HAH. The process consists of four sections as illustrated in Fig. 6. A more detailed process flow diagram, with the main equipment, is given in Fig. S10. The models for each of the sections were developed using Aspen Plus (V10 Aspen Technology). While the models for HMF production, HAH production and HAH purification sections are based on experimental results, flash columns in solvent recovery section are simulated using Aspen. In the HMF production section, the yields of HMF, HA, and byproducts from fructose are 85.9%, 2.7%, and 9.3%, respectively. Although the byproducts consist of several components, for simplicity, all the byproducts are labeled as humins. The HMF production reactor (R-1) is operated at 393 K and 10 bar so that all the components are in liquid phase. The stream exiting the reactor then enters the solvent recovery section, where it is passed through a throttling valve into a flash drum (S-1). Due to the reduction in pressure, a fraction of acetone/water is recovered as vapor and recycled to the HMF production section. The liquid outlet of the flash drum is then sent to an adsorption column (S-2), where activated carbon selectively adsorbs humins. Following the separation of humins, the stream enters a vacuum flash column (S-3), where more solvent is recovered in the vapor phase. Before recycling the vapor stream to the HMF production section, the vapor stream is liquified using a refrigerant available at 248 K. The evaporator operates at 293 K. This allows us to meet the required ratio of HMF to HA and acetone that is desirable for aldol-condensation reaction $\left(\frac{HMF}{Acetone + HA} = 2.5 \text{ on mole basis}\right)$. Following the solvent recovery section, HMF is converted to HA and HAH in the aldol-condensation reactor (R-2) in the presence of sodium hydroxide in 3.3% and 86.3% molar yields, respectively. While NaOH is a catalyst for aldol-condensation, acetone acts as both a reactant and solvent. Water, acetone, and NaOH are added such that the concentrations of HMF, acetone, and NaOH at the reactor throat are 655 mM, 325 mM, and 210 mM, respectively. In the HAH purification section, first HCl is added to neutralize NaOH. Thereafter, HAH is purified in a filtration tank (S-4), where it is precipitated and the remaining components including unreacted fructose and HMF, acetone, and HA dissolve in water and are sent to the wastewater treatment facility. Finally, the HAH cake contains some water and it is dried by circulating filtered hot air in a dryer (S-5). Then, we simulate a base design case with a fructose feedstock flow rate of 10,000 kg·h^{-1}. The mass and energy balances, temperature and pressure conditions of key process streams are given in Table S2.

Second, we optimize energy usage by performing heat integration using Aspen Energy Analyzer (V10 Aspen Technology). Without heat integration, the total heat required is 30 MW, and the total cooling required is 30.5 MW. Vacuum evaporator consumes almost half of the total required energy for heating and the condenser that liquifies acetone/water vapor stream from vacuum evaporator expends 60% of the total cooling requirements. Finally, the electricity requirement of the process is estimated to be 48.1 kW. Energy recovery of 6.2 MW is obtained (Table S3) by heat integration of the stream exiting S-1 and the stream entering S-3. It is assumed that the required electricity, heating and cooling are satisfied by external sources.

Third, equipment sizes and the corresponding costs are estimated. The costs of the reactors, filtration tank, adsorption columns and dryer are estimated using the cost data in the NREL report[31]. The costs of the remaining equipment are estimated using Aspen Process Economic Analyzer (V10 Aspen Technology). All the equipment and material costs are adjusted to a common year (2018) using appropriate cost indices. The capital and operating costs are summarized in Table S4 and S5, respectively. Total capital investment is computed to be $30.3 million and the operating cost is estimated to be $86.06 million/year.

Fourth, we calculate the minimum selling price (MSP) of HAH using discounted cash flow analysis (economic parameters given in Table S6). The MSP is computed to be $1958 per ton of HAH for a plant with production capacity of 46 kton/year of HAH.

Conflicts of interest

Authors declare that there is no conflict of interest.

Acknowledgements

This material is based upon work supported in part by the Great Lakes Bioenergy Research Center, U.S. Department of Energy, Office of Science, Office of Biological and Environmental Research under Award Number DE-SC0018409 and in part by U.S. Department of Energy under Award Number DE-EE0008353. We thank the Mass Spectrometry and NMR facilities that are funded by: Thermo Q ExactiveTM Plus by NIH 1S10 OD020022-1; Bruker Quazar APEX2 and Bruker Avance-500 by a generous gift from Paul J. and Margaret M.

Bender; Bruker Avance-600 by NIH S10 OK012245; Bruker Avance-400 by NSF CHE-414 1048642 and the University of Wisconsin-Madison. We thank Minsoo Ju for help in NMR analysis of HAH dimer.

Notes and references

1 S. Nishimura, N. Ikeda and K. Ebitani, in *Catalysis Today*, Elsevier, 2014, vol. 232, pp. 89–98.

2 B. Saha and M. M. Abu-Omar, *ChemSusChem*, 2015, **8**, 1133–1142.

3 A. Villa, M. Schiavoni, S. Campisi, G. M. Veith and L. Prati, *ChemSusChem*, 2013, **6**, 609–612.

4 A. F. Sousa, C. Vilela, A. C. Fonseca, M. Matos, C. S. R. Freire, G.-J. M. Gruter, J. F. J. Coelho and A. J. D. Silvestre, *Polym. Chem.*, 2015, **6**, 5961–5983.

5 A. H. Motagamwala, K. Huang, C. T. Maravelias and J. A. Dumesic, *Energy Environ. Sci.*, 2019, **12**, 2212–2222.

6 S. G. Wettstein, D. M. Alonso, Y. Chong and J. A. Dumesic, *Energy Environ. Sci.*, 2012, **5**, 8199.

7 S. G. Wettstein, J. Q. Bond, D. M. Alonso, H. N. Pham, A. K. Datye and J. A. Dumesic, *Appl. Catal. B Environ.*, 2012, **117–118**, 321–329.

8 E. I. Gürbüz, J. M. R. Gallo, D. M. Alonso, S. G. Wettstein, W. Y. Lim and J. A. Dumesic, *Angew. Chemie Int. Ed.*, 2013, **52**, 1270–1274.

9 J. S. Luterbacher, J. M. Rand, D. M. Alonso, J. Han, J. T. Youngquist, C. T. Maravelias, B. F. Pfleger and J. A. Dumesic, *Science*, 2014, **343**, 277–280.

10 D. M. Alonso, S. G. Wettstein and J. A. Dumesic, *Green Chem.*, 2013, **15**, 584–595.

11 J. Q. Bond, D. M. Alonso, D. Wang, R. M. West and J. A. Dumesic, *Science*, 2010, **327**, 1110–1114.

12 D. J. Braden, C. A. Henao, J. Heltzel, C. C. Maravelias and J. A. Dumesic, *Green Chem.*, 2011, **13**, 1755–1765.

13 J. C. Serrano-Ruiz, D. Wang and J. A. Dumesic, *Green Chem.*, 2010, **12**, 574–577.

14 Z. Hao and A. Iqbal, *Chem. Soc. Rev.*, 1997, **26**, 203–213.

15 T. Takeichi, T. Kano and T. Agag, *Polymer*, 2005, **46**, 12172–12180.

16 S. K. Burgess, D. S. Mikkilineni, D. B. Yu, D. J. Kim, C. R. Mubarak, R. M. Kriegel and W. J. Koros, *Polymer*, 2014, **55**, 6861–6869.

17 S. K. Burgess, D. S. Mikkilineni, D. B. Yu, D. J. Kim, C. R. Mubarak, R. M. Kriegel and W. J. Koros, *Polymer*, 2014, **55**, 6870–6882.

18 G. W. Huber, J. N. Chheda, C. J. Barrett and J. A. Dumesic, *Science*, 2005, **308**, 1446–1450.

19 H. Chang, A. H. Motagamwala, G. W. Huber and J. A. Dumesic, *Green Chem.*, 2019, **21**, 5532–5540.

20 T. W. Walker, A. K. Chew, H. Li, B. Demir, Z. C. Zhang, G. W. Huber, R. C. Van Lehn and J. A. Dumesic, *Energy Environ. Sci.*, 2018, **11**, 617–628.

21 S. K. R. Patil and C. R. F. Lund, *Energy & Fuels*, 2011, **25**, 4745–4755.

22 S. K. R. Patil and C. R. F. Lund, *Energy & Fuels*, 2011, **25**, 4745–4755.

23 M. J. McGrath, I. F. W. Kuo, B. F. Ngouana W., J. N. Ghogomu, C. J. Mundy, A. V. Marenich, C. J. Cramer, D. G. Truhlar and J. I. Siepmann, *Phys. Chem. Chem. Phys.*, 2013, **15**, 13578–13585.

24 R. M. West, Z. Y. Liu, M. Peter, C. A. Gärtner and J. A. Dumesic, *J. Mol. Catal. A Chem.*, 2008, **296**, 18–27.

25 S. P. Moulik, D. Basu and P. K. Bhattacharya, *Carbohydr. Res.*, 1978, **63**, 165–172.

26 J. Rorrer, S. Pindi, F. D. Toste and A. T. Bell, *ChemSusChem*, 2018, **11**, 3104–3111.

27 J. Rorrer, Y. He, F. D. Toste and A. T. Bell, *J. Catal.*, 2017, **354**, 13–23.

28 B. R. H Peters and H. H. Sumner, *J. Chem. Soc.*, 1953, 2101–2110.

29 ICIS, Asia Chemicals Outlook, 2019.

30 Changzhou AoZun Composite Material Co. Ltd., https://www.alibaba.com/product-detail/Best-Price-Dispersed-Anthraquinone-Price_60575920022.html?spm=a2700.7724857.normalList.47.4f1d58d0E7VUz8.

31 R. Davis, N. Grundl, L. Tao, M. J. Biddy, E. C. D. Tan, G. T. Beckham, D. Humbird, D. N. Thompson and M. S. Roni, *Tech. Rep. NREL/TP-5100-71949*.

Table of contents

Catalytic strategy for conversion of fructose to organic dyes, polymers, and liquid fuels

Hochan Chang[a], Ishan Bajaj[a], George W. Huber[a], Christos T. Maravelias[a], and James A. Dumesic*[a,b]

[a] Department of Chemical and Biological Engineering, University of Wisconsin-Madison, Madison, WI 53706, USA.

[b] DOE Great Lakes Bioenergy Research Center, University of Wisconsin-Madison, 1552 University Ave, Madison, WI 53726, USA.

* Corresponding author: James A. Dumesic (jdumesic@wisc.edu)

One sentence summary:

Catalytic pathway for supplying sustainable organic dyes, polymers, and liquid fuels from fructose by production of a versatile platform chemical